Anomalous cage effect in the excited state dynamics of catechol in the 18C6-catecol host-guest complex

Fumiya Morishima, Ryoji Kusaka, Yoshiya Inokuchi, Takeharu Haino and Takayuki Ebata*

Department of Chemistry, Graduate School of Science,

Hiroshima University, Higashi-Hiroshima 739-8526, Japan

Abstract

We present the structure of 18C6-catechol host-guest complex and the effect of the complexation on the S_1 dynamics of catechol studied under a supersonically cooled gas phase condition and in cyclohexane solution. In the gas phase bare catechol, two adjacent OH groups have an intramolecular hydrogen-bonded structure. On the other hand, in the 18C6-catechol (1:1) complex both of the catechol OH groups are hydrogen-bonded to the oxygen atoms of 18C6. This complex formation greatly changes the character of the S_1 state of catechol. That is, the S_1 lifetime of bare catechol is reported to be 7 ps, while the 18C6-catechol complex was obtained to be 10.3 ns. This anomalous S_1 lifetime elongation of catechol upon the complexation is attributed to a large energy gap between the S_1 ($\pi\pi^*$) and S_2 states by the switching from the intramolecular hydrogen-bond to the intermolecular hydrogen-bond in the host-guest complex. The formation of the18C6-catechol complex formation was also confirmed in cyclohexane solution, and an anomalous increase of fluorescence quantum yield of catechol was also observed. From the concentration dependence of the fluorescence intensity, it was confirmed that 18C6 and catechol also form (1:1) host-guest complex in bulk system. An equilibrium constant for the$18C6 + \text{catechol} \rightleftarrows 18C6 \cdots \text{catechol}$ reaction was obtained. It is suggested that that 18C6 can act as a sensor of detecting catechol.

1. Introduction

Catechol (pyrocatechol, 1, 2-benzenediol) is the ortho-substituted phenol with an extra OH group and the adjacent two OH groups form the intramolecular hydrogen (H)-bond (see scheme 1). The structure of catechol and its complexes in the electronic ground (S_0) and excited (S_1) states have been investigated extensively in the gases phase[1-8]. According to these studies, all atoms are located in the same plane of the aromatic ring and the molecule has C_s symmetry in the ground state of monomer. In contrast, in the S_1 state, the two OH groups are twisted out-of-plane of the benzene ring[2, 3, 5], and the symmetry of catechol is lowered to C_1.

The electronic excited state dynamics of catechol is also investigated by many researchers[9-11], because catechol has a rather short S_1 lifetime (7-12ps) compared to other similar aromatic molecules containing heteroatoms such as phenol, resorcinol and hydroquinone[9-13]. This very short lifetime is explained by a non-radiative mechanism similar to phenol. That is, phenol undergoes non-radiative decay from the optically allowed $S_1(\pi\pi^*)$ to the repulsive $S_2(^1\pi\sigma^*)$ state via conical intersection, and generates an H atom and phenoxy radical.[14-18] Catechol also relaxes through the similar route and releases the H atom from the ^{b}OH group free from H-bond.[10] The crucial difference between catechol and phenol is the specifically smaller $\pi\pi^*$ and $\pi\sigma^*$ energy gap due to the intramolecular H-bond.[9] In addition, the symmetry of catechol is lowered to C_1 in S_1. The smaller $\pi\pi^*/\pi\sigma^*$ energy gap and the lower symmetry leads to the anomalously fast nonradiative decay to $^1\pi\sigma^*$ in catechol.

In present study, we investigate the structure of 18C6-catechol host-gest complex and the cage effect on the S_1 dynamics of catechol by forming the complex. 18C6 is a well-known host species in the host-guest chemistry. In our previous study,[19] we investigated the structure of gas phase cold 3*n*C*n*-phenol complexes (n = 5 – 8) in supersonic free jets and found that 18C6-phenol complex forms a single unique isomer, while other complexes with different size of crown ethers form several isomers even under the supersonically cooled condition. The formation of the single

isomer of 18C6-phenol was described by the best matching of phenol and the flexible 18C6 cavity. Here, we extend that work to the 18C6-catechol complex. In bare catechol, the two OH groups form intramolecular hydrogen (H)-bond (intra-H-bond) (scheme 1). This intra-H-bond may be broken in the 18C6-catechol due to the formation of intermolecular hydrogen-bond (inter-H-bond) with ether oxygen(s) of 18C6. Such the external effect will affect the photo-physics of catechol. In this study, gas phase catechol and its complexes are generated under cold condition using a molecular beam technique. Several laser spectroscopic methods are applied to measure the electronic and IR spectra. The complex structures were determined from the observed IR spectra and quantum chemical calculation. The S_1 lifetime of the 18C6-catechol complex was obtained by convolution of fluorescence decay. In addition, we measured the S_1 lifetime of catechol monomer and catechol-H_2O complex by picosecond pump-probe spectroscopy. We will discuss how the complexation with 18C6 changes the conformation of catechol and its S_1 state dynamics. In addition to the gas phase study, we also investigated the complex formation in cyclohexane solution. We observed the anomalous increase of fluorescence quantum yield of catechol by the addition of 18C6 to catechol in cyclohexane solution. From the concentration dependence of the fluorescence intensity, it was confirmed that 18C6 and catechol also form 1:1 host-guest complex in bulk system. The result suggests an application of 18C6 as a tracer of catechol.

2. Experimental & computational

2-1. Gas phase experiment

Details of the experimental setup were described elsewhere.[20] In brief, jet-cooled catechol and 18C6-catechol complex were generated by employing the supersonic expansion of gaseous mixture of 18C6 and catechol with He carrier gas. 18C6 and catechol, both of which are solid crystal, were independently heated to vaporize in different sample housings and the 18C6/catechol gas mixture diluted with He at total pressure of 3-4 bar was expanded in a vacuum chamber through a 1 mm orifice of the pulsed nozzle. We applied LIF spectroscopy to obtain the S_1-S_0 electronic spectra. A tunable UV light obtained by second harmonics generation (SHG) of an output of the Nd^{3+}:YAG laser pumped dye laser (Lambda Physik Scanmate/Continuum Surelite II) was introduced into the vacuum chamber to cross the supersonic jet at ~30 mm downstream of the orifice. LIF spectra were obtained by detecting the total fluorescence as a function of UV frequency. We also performed UV-UV hole-burning (HB) spectroscopy[21] to discriminate a peak belonging to a different isomer; the frequency of the probe UV laser was fixed to a certain vibronic band of a specific species and its fluorescence intensity was monitored. Under this condition, another tunable UV laser (pump laser) light obtained by SHG of the Nd^{3+}:YAG laser pumped dye laser (Continuum ND6000 /Surelite II) was introduced at 10 mm upstream of the crossing point between the jet and the probe laser with a timing of ~4 μs prior to the probe laser pulse. The frequency of the UV hole laser was scanned and depletion of the fluorescence intensity induced by the absorption of the pump laser was observed. Thus, the UV-UV HB spectrum is obtained as a fluorescence-dip spectrum. The experimental scheme of IR-UV double resonance (DR) spectroscopy for measuring IR spectra is very similar to HB spectroscopy. Instead of UV laser, an output of a pulsed tunable IR laser (Laser Vision/Quanta-Ray GCR250) was employed as a pump laser. The IR laser is introduced coaxially to the probe UV pulse with a timing of 80 ns prior the UV pulse. UV probe laser frequency was fixed to certain vibronic band and the IR laser frequency was scanned. A depletion of the fluorescence

induced by the IR pump laser was observed, giving fluorescence-dip IR spectra for the UV monitored species. The S_1 lifetime of 18C6-catechol complex was obtained by convoluting the time profiles of the fluorescence decay curve with assuming laser pulse shape as a Gaussian function with 5.0 ns pulse width. In addition, we measured the S_1 lifetime of catechol and catechol-H_2O complex by pump-probe experiment with a picosecond laser system. The setup of the picosecond laser system has been also described in detail elsewhere.[22, 23] Briefly, two tunable picosecond UV laser pulses were obtained by SHG of two optical parametric generation/optical parametric amplifier (OPG/OPA) systems (Ekspra PG401 SH) pumped by a mode-locked picosecond Nd:YAG laser (Ekspra PL2143S). The spectral resolution of the UV laser was 5 cm^{-1} and the time resolutions of the two lasers were estimated to be 12 ps. The two lasers are introduce to a molecular beam machine, and crossed the molecular beam in a counter-propagated manner with each other. The lasers ionized the molecule or complex in the molecular beam by stepwise two-photon ionization. The ions were mass-analyzed with a 50 cm time-of-flight tube and were detected by a channeltron (Burle 4900). The decay time profiles of the S_1 state were obtained by measuring pump–probe ion signals as a function of the delay time between the pump UV and probe UV laser pulses, which was controlled with an optical delay line. The ion signals were processed by a boxcar integrator (Par model 4401/4420) connected by a personal computer. The decay time constants were obtained by convolution method. All the decay curves were fitted as a single exponential decay. 18C6 and catechol were purchased from SIGMA-ALDRICH and NACALAI TESQUE respectively and used without further purification.

2-2. Computational

To obtain the possible structure of the 18C6-catecol complex, we first used a classical force field to search initial conformations. We performed a Monte Carlo simulation by mixed torsional search with low-mode sampling[24] in MacroModel V.9.1[25] with MMFF94s force field,[26] and

optimized the geometries by PRCG algorithm with a convergence threshold of 0.05 kJ/mol. From this calculation, 193 isomers for 18C6-catechol complex were obtained within 20 kJ / mol. All these isomers were optimized by DFT calculation at the M05-2X / 6-31+G* level with *loose* optimization criteria. Then, 61 isomers were obtained within 20 kJ / mol. These 61 isomers were re-optimized at the ωB97X-D/6-31++G** level with *tight* optimization criteria and *ultrafine* grid. To obtain calculated IR spectra and electronic transition energies, we performed vibrational analysis and TD-DFT calculation at the same level in the final step. All DFT calculations are performed by Gaussian 09 package Revision D.01.[27] The OH stretching frequencies and electronic transition energies are scaled by 0.9325 and 0.8598, respectively, to reproduce the observed OH stretching vibration frequencies and the S_1-S_0 transition energy of catechol monomer.

2-3. Liquid phase experiment

The UV absorption spectra of pure catechol and catechol/18C6 mixture were measured in cyclohexane solution at the concentration of 5.3×10^{-4} mol / L. Fluorescence spectrum was measured for the catechol/18C6 mixture in cyclohexane solution by changing the concentration ratio of catechol : 18C6 from 1 : 0 to 9, where the concentration of catechol was fixed at 1.0×10^{-4} mol / L. This low concentration ensures non-aggregation of molecules in cyclohexane. Absorption spectra were measured with Hitachi U-3010 spectrophotometer and fluorescence spectra were measured with Hitachi F-2500 fluorescence-spectrophotometer. In addition, we measured fluorescence lifetime of catechol and 18C6-catechol mixture in cyclohexane solution. The fluorescence lifetime measurement was carried out with HORIBA Tem Pro1. The diode laser used for the excitation emits 250 nm light with a pulse width of 1.2 ns.

3. Results

3-1. Gas Phase experiment

Figure 1(a) shows LIF spectrum of jet-cooled catechol in the S_1-S_0 band origin region without adding 18C6. In the spectrum, band ***m*** at 35695 cm^{-1} is assigned to the (0,0) band of catechol monomer and band ***w*** at 35506 cm^{-1} to the 1:1 catechol-H_2O complex.[3] The appearance of catechol-H_2O complex is due to some residual water in catechol sample. The intensity of band ***m*** is very weak in the LIF spectrum because of the low fluorescence quantum yield due to the short S_1 lifetime of catechol,[11] while the band of catechol-H_2O (***w***) appears much stronger. The band located at 20 cm^{-1} higher frequency of band ***w*** is the intermolecular vibration. Figure 1(b) shows LIF spectrum measured by expanding an 18C6/catechol vapor mixture. In the spectrum, there are two prominent bands at 35230 cm^{-1} (band **I**) and 35548 cm^{-1} (band **II**). The red-shift of these bands from the band origin of bare catechol are 465 cm^{-1} for band **I** and 147 cm^{-1} for band **II**. These bands can be assigned to the 18C6-catecol complexes. Similar to the catechol-water complex, the complex bands appear much stronger than the monomer band. The results of UV-UV HB spectra in Figure 1(c) indicate that bands **I** and **II** belong to different 18C6-catechol complex with each other.

Figures 2(b) and(c) display the IR-UV DR spectra in the OH stretching vibrational region for bands **I** and **II**. Table 1 lists the frequencies of the observed OH stretching bands together with those of catechol and catechol-H_2O. The IR spectrum of catechol monomer (band **m**) could not be measured because of the weak LIF intensity. So, we compare the reported IR spectrum of catechol[6] in Fig. 2(a). In Fig. 2(a), the band at 3611 cm^{-1} is assigned to the stretching vibration of donor OH in the intra-H-bond (^{a}O-H$\cdots^{b}$O). The band at 3673 cm^{-1} is the acceptor OH (^{b}OH) [6]. The OH stretching bands in the 18C6-catechol complex in Figs. 2(b) and (c) appear in the 3350 – 3450 cm^{-1} region. The IR spectrum of band **I** (Fig. 2(b)) shows two OH stretching bands at 3384 and 3406 cm^{-1}. On the other hand, the IR spectrum of band **II** (Fig. 2(c)) shows only one band at 3423 cm^{-1}. In neither spectrum (b) nor (c), no band is seen in the 3600 -3700 cm^{-1} region, indicating no free OH nor

intra-H-bonded OH in these complexes. For the complex in which the intra-H-bond is still preserved, the position of the intra-H-bonded OH stretch is not so different from that of monomer. For example, the frequency of the intra-H-bonded OH stretch of catechol-H_2O is reported to be 3597 cm^{-1}. The frequency is only 14 cm^{-1} lower than that of bare catechol[6]. So, we conclude that in species **I** and **II**, both the two OH groups are H-bonded to ether oxygen atoms of 18C6. Under the experimental condition, we do not see the bands attributed to $(catechol)_2$ in the LIF spectrum. So from this experimental condition and the number of appeared OH stretching vibrational bands, we conclude that both the species **I** and **II** are due to the 18C6-catechol (1:1) complex. As will be discussed later, the reason of the appearance of the one OH stretch band in the IR spectrum for species **II** (Fig. 2(c)) is the overlap of the two OH bands.

The lifetime of catechol in the gas phase at the S_1 origin is reported as 7.0 – 8.7 ps.[10, 11] In the present study, we measured S_1 lifetime of bare catechol, catechol-H_2O (1:1) complex and 18C6-catecol (1:1) complex. The results obtained by picosecond pump–probe experiment for the catechol and catechol-H_2O (1:1) complex are displayed in Fig. 3(a). By fitting the time profiles with a single exponential decay, the S_1 lifetime of catechol was obtained to be 8.0 ps, which is consistent with the reported value.[10, 11] The S_1 lifetime of catechol-H_2O was obtained to be 2.0 ns. Thus, the inter-H-bonding to ^{b}OH elongates the S_1 lifetime of catechol. For the 18C6-catecol (1:1) complex, the S_1 lifetime was too long to be obtained by the picosecond pump–probe spectroscopic measurement, so we obtained the lifetime from the fluorescence decay curve. The results are shown in Figs. 3(b) and (d) for bands **I** and **II**. Convolution of the decay profiles with the laser pulse width of 5.0 ns and by assuming a single exponential decay gives the fluorescence lifetime of the species of bands **I** and **II** to be 10.3 ns for both species. Thus, the S_1 lifetime of catechol increases by more than three orders of magnitudes in the 18C6-catechol (1:1) complex. Thus, the inter-H-bonding to the two OH groups dramatically change the photophysics of catechol.

3-2. Liquid phase experiment

3-2-1. Absorption and fluorescence spectra

The 1:1 complex between 18C6 and catechol would also exist in the bulk system. So, we investigated the complex by measuring UV absorption and fluorescence spectra for the 18C6/catechol mixture in cyclohexane solution. Figure 4 shows UV absorption spectra of catechol (Red) and 1:1 mixture of catechol and 18C6 (Blue) in cyclohexane with the catechol concentration [catechol] =5.3×10^{-4} mol / L at room temperature. The two spectra are very similar except for the 1:1 mixture spectrum shows slight increase of the absorption intensity in the 34500-38000 cm^{-1} region. Then the fluorescence spectra were measured by exciting the sample at 280 nm (35,700 cm^{-1}). Figure 5 exhibits fluorescence spectra of catechol and catechol/18C6 mixture by changing the 18C6 concentration [18C6], so that the ratio [catechol] / [18C6] changes from 0.0 to 9.0. Here, catechol concentration is fixed at [catechol] = 1.0×10^{-4} mol/L. Figure 6 shows the plots of the ratio of total fluorescence intensity of catechol vs [18C6] / [catechol]. The fluorescence intensity of catechol monotonically increases with [18C6] up to [18C6] / [catechol] = 9.0 and there is no sign to reach the plateau, indicating that catechol forms 1:1 complex with 18C6 and gains its fluorescence intensity by the complex formation.

3-2-2. Fluorescence lifetime measurement

Figure 7(a) (red circle) shows fluorescence decay of catechol in cyclohexane solution at [catechol] = 5.3×10^{-5} mol / L. The decay curve shows double exponential decay. The fast component (solid line) is obtained to be 218 ps and slow component (dashed line) to be 10 ns. The slow component is due to some impurity in cyclohexane and only the fast component is attributed to the catechol fluorescence. Since 218 ps is much shorter than the excitation laser pulse width of 1.2 ns, this value gives only an upper limit of the measurable lifetime. As was described above, the fluorescence lifetime of gas phase catechol is reported to be 7. 0 ps and the fluorescence lifetime in

cyclohexane solution may not be so different from the gas phase value. Figs. 7(b) and (c) show fluorescence decay curve of 18C6/catechol mixture in cyclohexane solution measured at [catechol] / [18C6] ratio of (b) 0.28 and (c) 0.67. Convolution of the decay curves with the laser time profile gives the lifetime of 1.83 ns for (b) and 1.94 ns for (c). Based the uncertainty of the values, the two values are essentially the same and we think the observed lifetime is attributed to the 18C6-catecol 1:1 complex formed in solution. Thus, it is concluded that 18C6 and catechol form 1:1 complex even in the bulk condition, and catechol highly gains its fluorescence quantum yield by forming the complex.

4. Discussion

4-1. Structure of the18C6-catechol 1:1 complex

Figure 8 shows the calculated lowest energy structures of 18C6-catechol (1:1) complex within the energy of 10 kJ / mol. In this energy, seven isomers were obtained and they can be classified into two types, **Type-1** and **Type-2,** according to the H-bonding pattern. The relative energies, OH stretching frequencies, and dihedral angles of the two OH groups of catechol are also listed in Table 1.

Type-1 (Structures **A1** and **A2**) : Catechol preserves the ^{a}O-H$\cdots^{b}$O intra-H-bond, and ^{b}O-H forms the inter-H-bond with an oxygen atom of 18C6. This is a similar structure with that of catechol-H_2O 1:1 complex.[3, 6] Structure **A1** is most stable and **A2** has almost same energy.

Type-2 (Structures **E1-E5**) : In these isomers, the ^{a}O-H$\cdots^{b}$O intra-H-bond is broken. The two OH groups of catechol are twisted out of benzene plane to the same direction by 20 – 30 degrees, and they are independently H-bonded to the oxygen atoms of 18C6. In these structures, 18C6 plays a role of cage for catechol. The energies of Type-2 isomers are higher than Type-1 isomers by more than ~4 kJ/mol at ωB97X-D / 6-31++G** level calculation.

Though Type-1 structure is energetically more favored than Type-2, the IR spectra give opposite result. Figure 2 (d) shows the calculated IR spectra of Type-1(**A1**, **A2**) and Type-2(**E1-E5**) isomers. In Type-1 isomers, the H-bonded OH (^{b}OH) stretching vibration appears at 3300-3350 cm^{-1} region, and the band of the intra-H-bonded ^{a}OH appears at 3580cm^{-1}. By comparing ^{a}OH of bare catechol, we see that the position of the intra-H-bonded ^{a}OH is not so affected even ^{b}OH forms the inter-H-bond. Either of the IR spectra of **A1** or **A2** does not reproduce the observed spectra of species **I** (Fig. 2(b)) or **II** (Fig. 2(c)). On the other hand, the calculated IR spectra of Type-2 structures show very similar spectral patterns with the observed ones. In these spectra, the two H-bonded OH stretching bands appear at 3350-3450 cm^{-1} with similar intensity. In **E1** and **E3** isomers, the two OH bands are separated, while in **E2, E4** and **E5,** the two OH stretching bands are

almost overlapped. Thus, the observed species **I** can be assigned either to **E1** or **E3**, and species **II** to either **E2**, **E4** or **E5**. As seen in Table 1, **E1** is 4. 2 kJ/mol more stable than **E3**, so species **I** may be assigned to **E1**. On the other hand, **E2**, **E4** and **E5** have similar energies with each other. So, we calculated S_1-S_0 transition energies of the complexes by TD-DFT calculation to obtain further information of the complexes. The calculated S_1-S_0 energies are listed in Table 2 together with the observed energies of bare catechol, catechol-H_2O. Among **E2, E4** and **E5,** the S_1-S_0 transition energy of **E4** shows smallest red-shift (577 cm^{-1}), while the shifts of other conformers are more or less the same (850-870 cm^{-1}). Thus, species **II** may be assigned to **E4** structure. We do not have a clear explanation why **E4** has the smaller change shift value but we considered it may arise from the smallest change of dihedral angles C1-C2-^{a}O-H3 or largest of C2-C4-^{b}O-H5 from those of monomer (see Table 1).

4-2. The elongation of S_1 lifetime in 18C6-catechol in gas phase

We found that the S_1 lifetime of 18C6-catechol complex (10.3 ns) is more than 1400 times longer than that of catechol monomer (7ps) and 5 times longer than catechol-H_2O complex (2.0 ns). Here we discuss the reason of the anomalous elongation of the S_1 lifetime of the 18C6-catechol complex. As was mentioned in introduction, the short S_1 lifetime of catechol monomer is attributed to the fast internal conversion to the S_2 ($^1\pi\sigma^*$) state due to a small S_1 ($\pi\pi^*$) – S_2 ($^1\pi\sigma^*$) energy gap compared to other molecules.[9, 10] So, the drastic elongation of the lifetime in the complex indicates an increase of the S_1 – S_2 energy gap compared to bare catechol. So, we calculated the S_1 and S_2 energies of catechol and complexes by TD-DFT calculation with a fixed geometry of S_0, and the results are listed in Table 2. In the supporting information (figure S1), the σ^* orbital of catechol and catechol-H_2O complex are shown. In catechol monomer, the energies of S_1 ($\pi\pi^*$) and S_2 ($^1\pi\sigma^*$) are 4.43 and 4.68 eV, respectively, so S_2 is located at 0. 25 eV higher than S_1. In the catechol-H_2O 1:1 complex, on the other hand, the difference is 0. 15 eV. This value is smaller than the monomer. This result seems to contradict to the experimental result that catechol-H_2O shows longer lifetime than monomer. This contradiction may be due to the insufficient level of calculation. It should be noted that even in the CASPT2 calculation by Sobolewski and Domcke, they obtained smaller S_1 ($\pi\pi^*$) - S_2 ($^1\pi\sigma^*$) energy gap in phenol-H_2O 1:1 complex than in phenol[28] although the S_1 lifetime of 1:1 phenol-H_2O complex (15 ns) is longer than phenol (2 ns).[13] As seen in Table 2, the S_2 state is located at 0.5 – 0.7 eV higher than S_1 in all 18C6-catechol complexes. This energy gap is twice of that of bare catechol and this larger gap will causes a larger barrier for the crossing of the potential curves of the two states, leading to the drastic long S_1 lifetime of the 18C6-catechol complex. I was found that the S_2 state of 18C6-catechol complex has more mixed electronic character different from catechol and catechol-H_2O complex. In the supporting information (figure S2), several orbitals involved in S_2 are shown for **E1** and **E4** isomers of 18C6-catechol complex. As seen in the figure, we

do not identify the σ* orbital of catechol site, so the energy of this orbital seems to be raised to higher energy in the complex.

289 **4-3. Equilibrium constants of the"$18C6 + \text{catechol} \rightleftarrows 18C6 \cdots \text{catechol}$" reaction in solution**

290 From the plot of fluorescence intensity vs. 18C6 concentration of Fig.6, we can obtain the
291 equilibrium constant of the "$18C6 + \text{catechol} \rightleftarrows 18C6 \cdots \text{catechol}$" reaction. The equilibrium
292 constant *K* of this reaction is expressed as,

$$K = \frac{[18C6 \cdots catechol]}{[catechol][18C6]}. \qquad (1)$$

293 Where, $[18C6 \cdots catechol]$ is concentration of $18C6 \cdots$ catechol complex under equilibrium
294 condition. By employing the complex formation probability α, (0<α<1), the equation (1) can be
295 rewritten as

$$K = \frac{\alpha[18C6]_0}{([catechol]_0 - \alpha[18C6]_0)\{(1-\alpha)[18C6]_0\}}. \qquad (2)$$

296 Here, $[catechol]_0$ and $[18C6]_0$ are the initial concentration. In the experiment, we obtained the
297 fluorescence intensities of the catechol (F_1) and the catechol-18C6 complex (F_2) vs. $[18C6]_0$ /
298 $[\text{catechol}]_0$ ratio,

$$\mathrm{F} = \mathrm{F}_1 + \mathrm{F}_2. \qquad (3)$$

300 By using an instrument dependent constant A, and fluorescence quantum yields, ϕ_{catechol} and
301 $\phi_{18C6-catechol}$, for each species,

$$\mathrm{F1} = A[\text{catechol}]\phi_{\text{catechol}} = \mathrm{A}([\text{catechol}]_0 - \alpha[18C6]_0)\phi_{\text{catechol}} \qquad (4a)$$

303 and

$$\mathrm{F2} = A[18C6 - catechol]\phi_{18C6-catechol} = A(\alpha[18C6]_0)\phi_{18C6-catechol}. \qquad (4b)$$

305 In Fig. 6, we plotted the Ratio

$$\text{Ratio} = \frac{\mathrm{F}_1 + \mathrm{F}_2}{\mathrm{F1}([18C6]_0 = 0)} = \frac{([catechol]_0 - \alpha[18C6]_0)\phi_{catechol} + \alpha[18C6]_0\phi_{catechol\cdots 18C6}}{[catechol]_0\phi_{catechol}}, \qquad (5)$$

306 as a function of $[18C6]_0$. Under the condition that relative concentration of the catechol-18B6 is
307 much lower than that of catechol, eq. (5) can be simplified as,

$$\text{Ratio} = 1 + \frac{\alpha\phi_{catechol\cdots 18C6}}{\phi_{catechol}}\frac{[18C6]_0}{[catechol]_0}. \qquad (6)$$

So, the ratio will be in proportional to the added 18C6 concentration, $[18C6]_0$. This condition is realized in the concentration range of $[18C6]_0$ / [catechol] $_0 < 2.0$ in Fig. 6. So, we obtained the slope to be

$$\frac{\alpha\phi_{catechol\cdots 18C6}}{\phi_{catechol}} = 5.5, \qquad (7)$$

by linear fitting of the plot of Fig. 6 in the range $[18C6]_0$ / [catechol] $_0$ = 0 - 2.0. The ratio of the fluorescence quantum yield, $\phi_{\text{catechol-18B6}} / \phi_{\text{catechol}}$, can be obtained by the fluorescence lifetime of catechol and the catechol-18C6 complex in solution, since the absorption intensity is not so different between them as seen in Fig. 4. The fluorescence lifetime of the catechol-18C6 complex was experimentally obtained to be 1. 9 ns. However, the lifetime of catechol in solution is too short to measure with our setup. So, we assume the lifetime would be the same with that of gas phase, 7 ps. By using this assumption, α is obtained to be $2.0\text{x}10^{-2}$. Finally, under the condition that relative concentration of the catechol···18B6 is much lower than that of catechol, eq. (2) can be simplified as

$$K = \frac{\alpha}{[catechol]_0}. \qquad (8)$$

Since we fixed $[\text{catechol}]_0 = 1.0\text{x}10^{-4}$ mol/L in Fig. 6, the equilibrium constant K is obtained to be 2.0 x 10^2 L / mol ($\log K = 2.31$). We compare this value with other reaction involving 18C6, such as $18C6 + M^{n+} \rightleftarrows 18C6 \cdots M^{n+}$. The equilibrium constant of this reaction is reported to be $\log K = 2.34$ for M= Li in acetonitrile solution at 300 K[29], 2.31 for Na^+ in methanol at 298 K[30], 2.42 for Hg^{2+} in water at 298 K[31], 2.44 for Nd^{3+} in methanol at 298 K[32]. For molecular cation, K = 2.37 for PhN_2^+ in methanol at 298 K[33]. So, the equilibrium constant of catechol···18B6 is comparable with them, indicating this complex very stable in cyclohexane solution even though it is neutral.

Conclusion

We investigated the structure of 18C6-catechol complex and the effect of the complex formation on the S_1 dynamics of catechol by employing supersonic expansion/laser spectroscopic methods and theoretical calculation. We found catechol forms a unique 1:1 H-bonded complex with 18C6 by breaking its intramolecular H-bond. This complex formation changes not only the conformation of catechol but also the photochemistry of catechol dramatically. In S_1, bare catechol dissociates to catechoxy radical and H atom via tunneling through an $S_1(\pi\pi^*)$ / $S_2(\pi\sigma^*)$ conical intersection with a lifetime of 7 ps. However, the intermolecular H-bonding of the two OH groups with the oxygen atoms of 18C6 raises the energy of S_2 by 0.5-0.7 eV and inhibits the dissociation process, resulting in the S_1 lifetime of 10.3 ns. This 1:1 complex was also observed in solution. Similar to the gas phase results, catechol largely gains its fluorescence quantum yield by forming complex with 18C6. The S_1 lifetime of the 18C6-catechol 1:1 complex was determined to the 1.9 ns in cyclohexane solution. The dependence of the fluorescence gain on 18C concentration indicates the generation of the 1:1 complex even in cyclohexane solution, and the equilibrium constant was determined to be $K = 2.0 \times 10^2$ L / mol. This unique 1:1 complex formation and drastic gain of the fluorescence quantum yield suggest that 18C6 can act as a tracer of catechol in solution.

Reference

1. Dunn, T. M.; Tembreull, R.; Jubman, D. M Free-Jet Spectra and Structure of *o*-, *m*- and *p*-Dihydroxybenzene. *Chem. Phys. Lett*. **1985**, *121*, 453-457.
2. Bürgi, T.; Leutwyler, S. O-H Torsional Vibration in the S_0 and S_1 States of Catechol. *J. Chem Phys.* **1994**, *101*, 8418-8429.
3. Gerhards, M.; Schumm, S. P.; Henrichs, U.; Jacoby, C.; Kleinermanns, K. Structure and Vibrations of Catechol and Catechol$H_2O(D_2O)$ in the S_0 and S_1 State. *J. Chem. Phys.* **1996**, *104*, 9362-9375.
4. Gerhards, M.; Schumm, S. P.; Henrichs, U.; Jacoby, C.; Kleinermanns, K. Structure and Vibrations of Catechol$(Methanol)_1$ in the S_0 and S_1 State. *J. Chem. Phys.* **1996**, *106*, 878-884.
5. Gerhards, M.; Schumm, S.; Unterberg, C.; Kleinermanns, K. Structure and Vibrations of Catechol in the S_1 and Ionic Ground state. *Chem. Phys. Lett.* **1998**, *294*, 65-70.
6. Gerhards, M.; Unterberg, C.; Kleinermanns, K. Structure of Catechol$(H_2O)_{1,3}$ Clusters in the S_0 and D_0 states. *Phys. Chem. Chem. Phys.* **2000**, *2*, 5538-5544.
7. Kjaergaard, G. H.; Howard, L. D.; Schofield, P.; Robinson, W. T.; Ishiuchi, S.; Fujii,. M. OH- and CH-Stretching Overtone Spectra of Catechol. *J. Phys. Chem. A*. **2002**, *106*, 258-266.
8. Ahn, D.; Jeon, I.; Jang, S.; Park, S.; Lee, S.; Cheong, W. Hydrogen Bonding in Aromatic Alcohol-Water Clusters: A Brief Review. *Bull. Korean. Chem. Soc*. **2003**, *24*, 695-702.
9. Livingstone, A. R.; Tompson, O. F. J.; Ilijina, M.; Donaldson, J. R.; Sussman, J. B.; Paterson, J. M.; Townsend, D. Time-Resolve Photoelectron Imaging of Excited State Relaxation Dynamics in Phenol, Catechol, Resorcinol and Hydroquinone. *J. Phys. Chem.* **2012**, *137*, 184304.
10. Chatterley, S. A.; Young, D. J.; Dave Townsend, D.; Żurek, M. J.; Paterson, J. M.; Roberts, M. G.; Stavros, G. V. Manipulating Dynamics with Chemical Structure: Probing Vibrationally-Enhanced Tunneling in Photoexcited Catechol. *Phys. Chem. Chem. Phys.* **2013**, *15*, 6879-6892.

11. Weiler, M.; Miyazaki, M.; Féraud, G.; Ishiuchi, S.; Dedonder, C.; Jovvet, C.; Fujii, M. Unusual Behavior in the First Excited State Lifetime of Catechol. *J. Phys. Chem. Lett*. **2013**, *4*, 3819-3823.
12. D. Young, D. J.; Staniforth, M.; Chatterley, S. A.; Paterson, J. M.; Roberts, M. G.; Stavros, G. V. Relaxation Dynamics of Photoexcited Resorcinol: Internal Conversion Versus H Atom Tunnelling. *Phys. Chem. Chem. Phys*. **2014**, *16*, 550-562.
13. Lipert, J. R.; Bermudez, G.; Colson, D. S. Pathways of SI Decay in Phenol, Indoles, and Water Complexes of Phenol and Indole a Free Jet Expansion. *J. Phys. Chem.* **1988**, *92*, 3801-3805.
14. Sobolewski, A. L.; Domcke, W.; Dedonder-Lardeux, C.; Jouvet, C. Excited-state hydrogen detachment and hydrogen transfer driven by repulsive $^1\pi\sigma^*$ states: A new paradigm for nonradiative decay in aromatic biomolecules. *Phys. Chem. Chem. Phys.* **2002**, *4*, 1093–1100.
15. Nix, G. D. M.; Devine, L A.; Cronin, B.; Dixon, N. R.; Ashfold, N. R. M.; High Resolution Photofragment Translational Spectroscopy Studies of the Near Ultraviolet Photolysis of Phenol. *J. Chem. Phys.* **2006**, *125*, 133318.
16. Vieuxmarie, P. J. O.; Lan, Z.; Sobolewski, L.A.; Domcke, W. Ab initio Characterization of the Conical Intersections Involved in the Photochemistry of Phenol. *J. Chem. Phys.* **2008**, *129*, 224307.
17. Ashfold, N. R. M.; King, A. G.; Murdock, D.; Nix, G. D. M.; Oliver, A. A. T.; Sage, G. A. $\pi\sigma^*$ Excited States in Molecular Photochemistry. *Phys. Chem. Chem. Phys*. **2010**, *12*, 1218–1238.
18. Pino, G. A.; Oldani, A. N.; Marceca, E.; Fujii, M.; Ishiuchi, S.-I.; Miyazaki, M.; Broquier, M.; Dedonder, C.; Jouvet, C. Excited state hydrogen transfer dynamics in substituted phenols and their complexes with ammonia: $\pi\pi^*$-$\pi\sigma^*$ energy gap propensity and ortho-substitution effect. *J. Chem. Phys.* **2010**, *133*, 124313.

19. Kusaka, R.; Inokuchi, Y.; Haino, T.; Ebata, T. Structures of (3n-Crown-n)−Phenol (n = 4, 5, 6, 8) Host−Guest Complexes: Formation of a Uniquely Stable Complex for n = 6 via Collective Intermolecular Interaction. *J. Phys. Chem. Lett*. **2012**, *3*, 1414−1420
20. Inokuchi, Y.; Kobayashi, Y.; Ito, T.; Ebata, T. Conformation of L-Tyrosine Studied by Fluorescence-Detected UV-UV and IR-UV Double-Resonance Spectroscopy. *J. Phys. Chem. A* **2007**, *111*, 3209-3215.
21. Lipert, R.J.; Colson, S.D. Persistent Spectral Hole Burning of Molecular Clusters in a Supersonic Jet *J. Phys. Chem.* **1989**, *93*, 3894-3896.
22. Yamada, Y.; Mikami, N.; T, Ebata. Relaxation Dynamics of NH Stretching Vibrations of 2-Aminopyridine and its Dimer in a Supersonic Beam. *Proc. Natl. Acad. Sci. U. S. A.* **2008**, *105*, 12690–12695.
23. Kusaka, R.; T. Ebata. Remarkable Site Difference of Vibrational Energy Relaxation in Benzene Dimer: Picosecond Time-Resolved IR–UV Pump–Probe Spectroscopy. *Angew. Chem., Int. Ed*. **2010**, *49*, 6989–6992.
24. Kolossváry, I.; Guida, W. C. Low Mode Search. An Efficient, Automated Computational Method for Conformational Analysis: Application to Cyclic and Acyclic Alkanes and Cyclic Peptides. *J. Am.Chem. Soc*. **1996**, *118*, 5011−5019.
25. MacroModel, version 9.1; Schro¨dinger, LLC: New York, 2005.
26. Halgren, T. A. MMFF VII. Characterization of MMFF94, MMFF94s, and Other Widely Available Force Fields for Conformational Energies and for Intermolecular-Interaction Energies and Geometries. *J. Comput. Chem.* **1999**, *20*, 730−748.
27. Gaussian 09, Revision D.01, Frisch, M. J.; Trucks, G. W.; Schlegel, H. B.; Scuseria, G. E.; Robb, M. A.; Cheeseman, J. R.; Scalmani, G.; Barone, V.; Mennucci, B.; Petersson, G. A. et al. Gaussian, Inc., Wallingford CT, 2009.
28. Sobolewski, L. A.; Domcke, W. Photoinduced Electron and Proton Transfer in Phenol and Its

Clusters with Water and Ammonia. *J. Phys. Chem. A* **2001**, *105*, 9275-9283.

29. Smetana, A. J.; Popov, A. I. Lithium-7 nuclear magnetic resonance and calorimetric study of lithium crown complexes in various solvents *J. Solution Chem.* **1980**, *9*, 183-196.
30. Lin. J. D.; Popov. A. I. Nuclear magnetic resonance studies of some sodium ion complexes with crown ethers and [2]-cryptands in various solvents. *J. Am. Chem. Soc.* **1981**, *103*, 3773-3777.
31. Izatt, R. M.; Terry, R. E.; Haymore, B. L.; Hansen, L. D.; Dalley, N. K.; Avondet, A. G.; Christensen, J. J. Calorimetric titration study of the interaction of several uni- and bivalent cations with 15-crown-5, 18-crown-6, and two isomers of dicyclohexo-18-crown-6 in aqueous solution at 25.degree.C and .mu. = 0.1 *J. Am. Chem. Soc.* **1976**, *98*, 7620-7626.
32. Izatt, R. M.; Lamb, J. D.; Christensen, J. J.; Haymore, B. L. Anomalous stability sequence of lanthanide(III) chloride complexes with 18-crown-6 in methanol. Abrupt decrease to zero from gadolinium(3+) ion to terbium(3+) ion *J. Am. Chem. Soc.* **1977**, *99*, 8344-8346.
33. Izatt, R. M.; Lamb, J. D.; Rossiter, B. E.; Izatt, N. E.; Christensen, J. J. Thermodynamics of formation of 18-crown-6 complexes with arenediazonium and anilinium salts in methanol at 25 °C. *J. Am. Chem. Soc. Chem. Commun.* **1978**, *9*, 386-387

Table 1 The dihedral angles of C1-C2-^{a}O-H3 and C2-C4-^{b}O-H5 (see scheme 1), relative energy of stable isomers of catechol, and observed and calculated frequencies of the OH stretching vibration of catechol and its complexes. The structural optimization and vibrational analysis are performed at the level of ωB97X-D / 6-31++G**.

	Dihedral angle [degree]		Relative energy [kJ / mol]	OH stretching freq.[cm^{-1}]	
	^{a}OH	^{b}OH		Obs	Calc‡.
bare catechol	~180	~180		3611† (^{a}OH), 3673† (^{b}OH)	3612 (^{a}OH), 3672 (^{b}OH)
catechol-H_2O	~180	~180		3597† (^{a}OH), 3499† (^{b}OH)	3599 (^{a}OH), 3499 (^{b}OH)
Isomer I				3385, 3407	
Isomer II				3424	
A1	179.4	178.6	0.00		3584, 3311
A2	178.9	163.5	0.92		3584, 3325
E1	151.0	159.5	3.94		3429, 3372
E2	164.8	149.4	7.45		3396, 3386
E3	162.4	151.5	8.12		3391, 3331
E4	169.6	139.5	8.66		3390, 3404
E5	162.7	146.4	9.25		3381, 3386

†According to Ref. 3.
‡All calculated OH stretching frequencies are scaled by 0.9325 so as to reproduce those of catechol monomer.

Table 2 Observed S_1-S_0 transition energies of catechol and its complexes with H_2O and 18C6, calculated energies of $S_1(\pi\pi^*)$ and S_2 states, and the oscillator strengths from S_0 state. TD-DFT calculation are performed at the level of ωB97X-D / 6-31++G**.

	S_1-S_0 transition energy [cm^{-1}]	Energy of state[eV] (Osc. strength)	
		S_1	S_2
bare catechol	35695	4.4256 (0.0507)	4.6820 (0.0004)
catechol-H_2O	35506	4.3937 (0.0531)	4.5446 (0.0005)
Isomer I	35230		
Isomer II	35548		
E1		4.3196 (0.0513)	5.0403 (0.0086)
E2		4.3185 (0.0669)	4.8721 (0.0047)
E3		4.3186 (0.0685)	4.8353 (0.0041)
E4		4.3541 (0.0554)	4.9928 (0.0181)
E5		4.3201 (0.0657)	4.8690 (0.0051)

Figure caption

Figure 1 (a) S_1-S_0 LIF spectrum of catechol and catechol-water in a supersonic free jet. (b) S_1-S_0 LIF spectrum of catechol-B18C6 in a supersonic free jet. (c) UV-UV HB spectra of 18C6-catechol (I and II) and catechol-H_2O complex

Figure 2 (a) IR spectra of catechol in the OH stretching region. The spectrum was reproduced by using reported frequencies and relative intensities. (ref. 6) (b) IR-UV DR spectra of 18C6-catechol for band I. (c) IR-UV DR spectra of 18C6-catechol for band II. (d) IR spectra of isomers A1,A2 and E1-E5 of 18C6-catechol obtained by DFT calculation.

Figure 3 (a) Pump-probe decay profiles of profile of bare catechol (band m), and catechol-H_2O (1:1) complex (band *w*). (b) Fluorescence decay curves of bands I and II of 18C6-catechol.

Figure 4 UV absorption spectra of pure catechol (Red) and 18C6/catechol (Blue) mixture in cyclohexane solution. In both solution, concentration of catechol is fixed at 5.3×10^{-4} mol / L.

Figure 5 UV fluorescence spectra of catechol at difference 18C6/catechol concentration ratio in cyclohexane solution. Here, the concentration of catechol is kept at 1.0×10^{-4} mol / L.

Figure 6 Plot of the total fluorescence intensity of catechol vs. 18C6/catechol concentration ratio. The intensities are normalized with respect the fluorescence intensity of pure catechol. The black line represents the liner fit in the range from [18C6] / [catechol] = 0 to 2.0 and the red curve represents the fitting used by Hill equation.

Figure 7 (Red) The fluorescence decay curves of (a) catechol, and 18C6/catechol mixture in cyclohexane solution at [catechol] / [18C6] ratio of (b) 0.28 and (c) 0.67. The black dashed curves are decay profiles of impurity in the cyclohexane solvent. The black solid curves are decay profiles of catechol obtained by subtracting the fluorescence decay of cyclohexane solvent from the total decay curve.

Figure 8 Seven lowest energy stable structures of 18C6-catechol isomers within the energy of 10 kJ / mol at ωB97X-D / 6-31++G** calculation level.

Scheme 1 conformation of catechol monomer and classification of two OH. The dashed line represents intramolecular H-bond (^{a}O-H$\cdots^{b}$O). The purple and green line exhibit two dihedral angle C1-C2-^{a}O-H3 and C2-C4-^{b}O-H5, respectively.

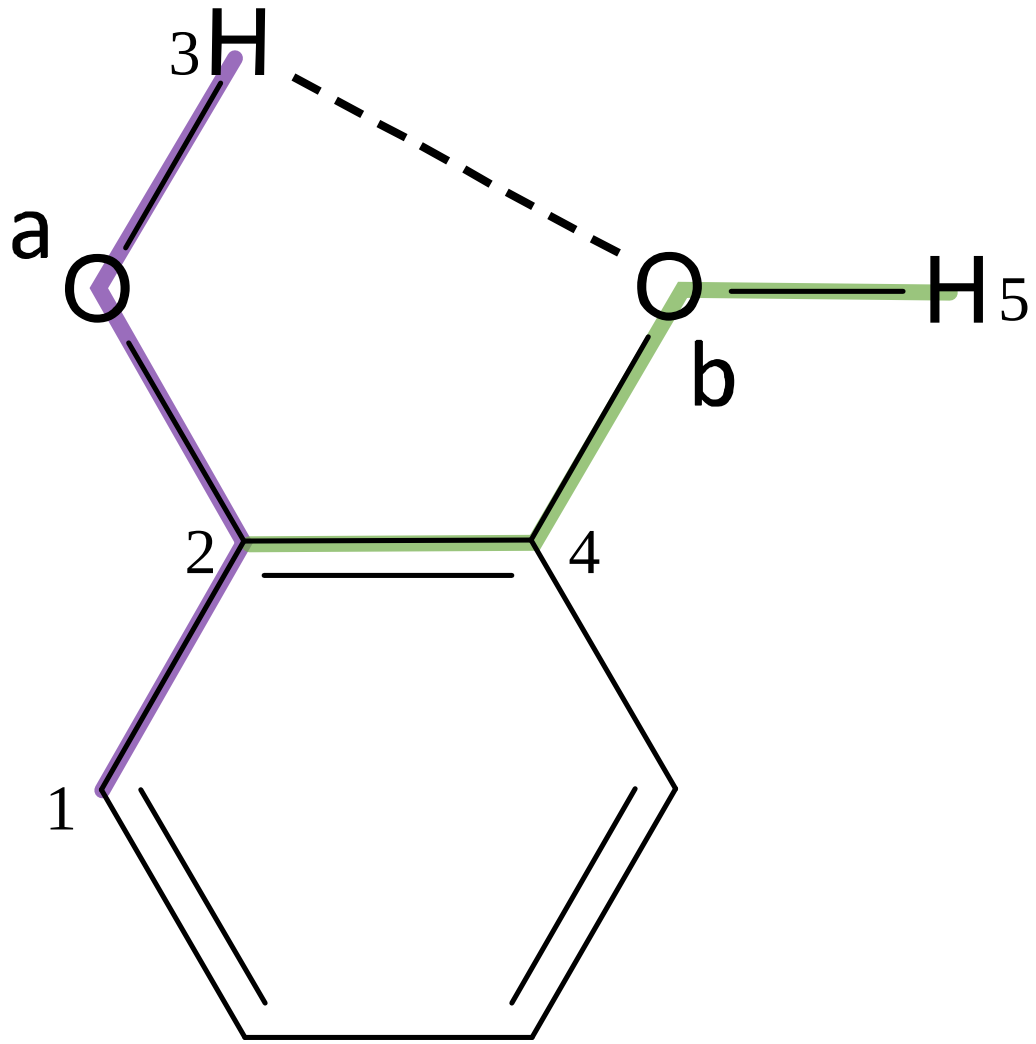

Figure 1

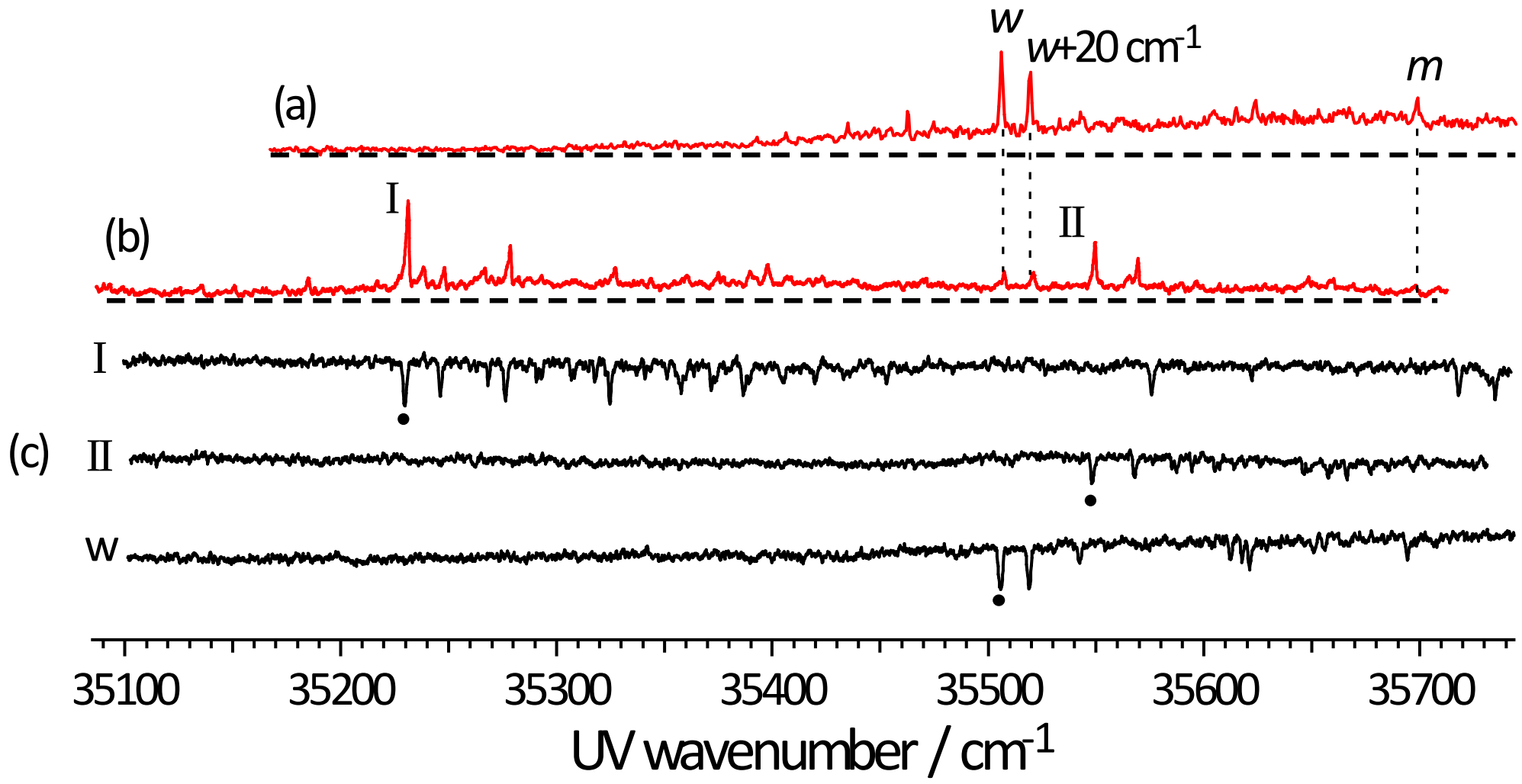
w
w+20 cm-1
m
(a)
I
(b)
II
I
(c)
II
w
35100
35200
35300
35400
35500
35600
35700
UV wavenumber / cm-1

Figure 2

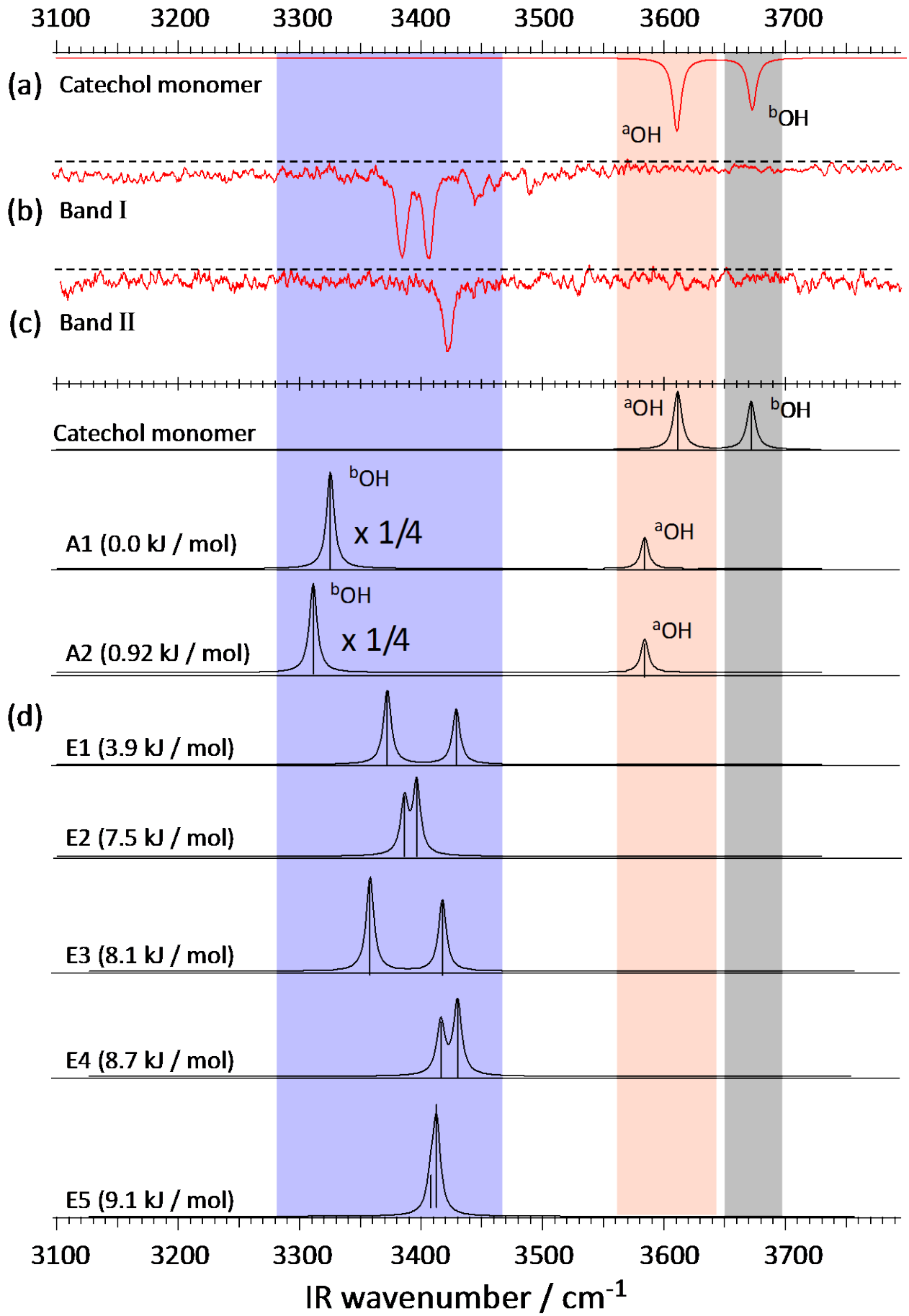
3100
3200
3300
3400
3500
3600
3700
(a) Catechol monomer
aOH
bOH
(b) Band I
(c) Band II
Catechol monomer
aOH
bOH
bOH
x 1/4
aOH
A1 (0.0 kJ / mol)
bOH
x 1/4
aOH
A2 (0.92 kJ / mol)
(d)
E1 (3.9 kJ / mol)
E2 (7.5 kJ / mol)
E3 (8.1 kJ / mol)
E4 (8.7 kJ / mol)
E5 (9.1 kJ / mol)
3100
3200
3300
3400
3500
3600
3700
IR wavenumber / cm-1

Figure 3

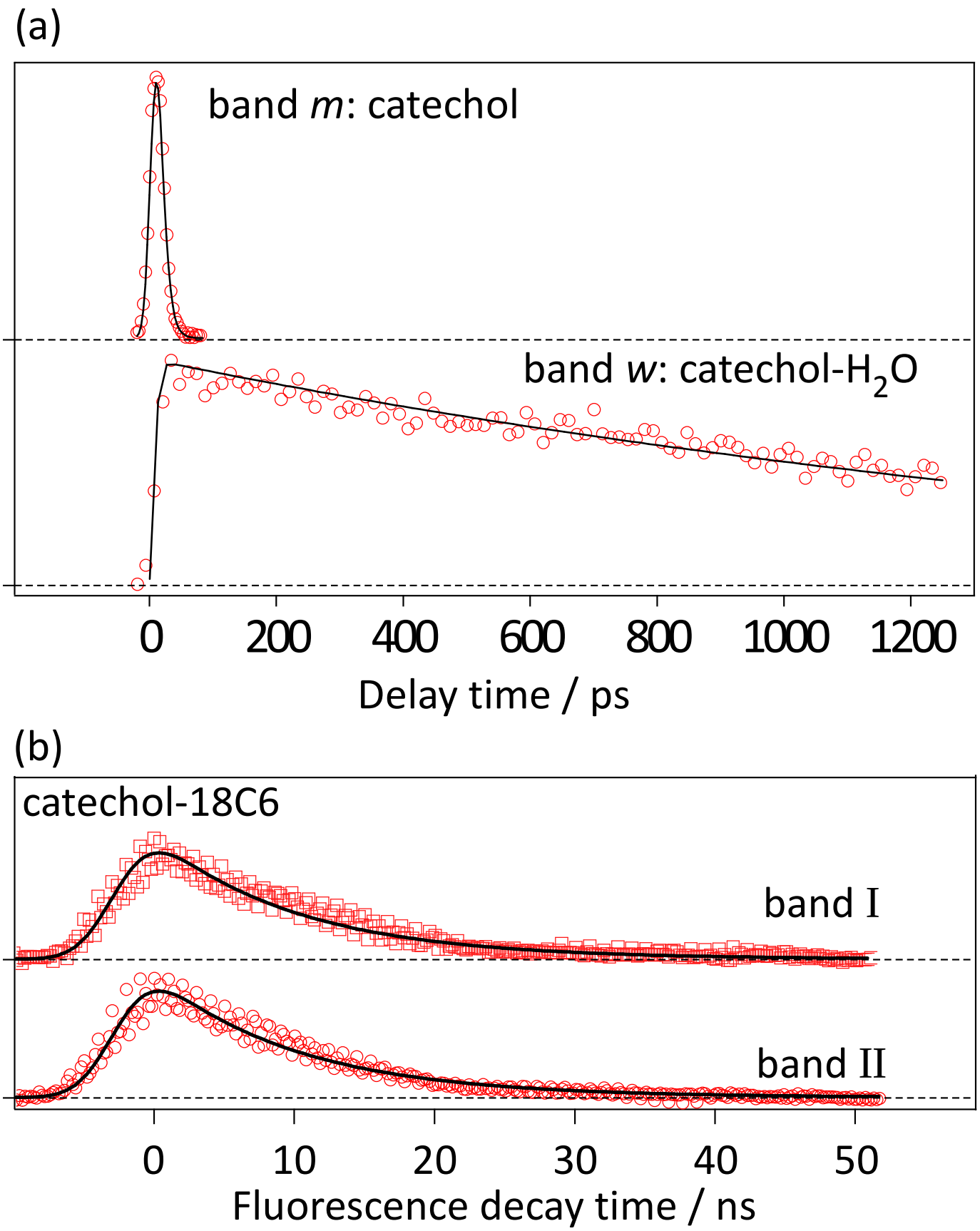
(a)
band m: catechol
band w: catechol-H2O
0
200
400
600
800
1000
1200
Delay time / ps
(b)
catechol-18C6
band I
band II
0
10
20
30
40
50
Fluorescence decay time / ns

Figure 4

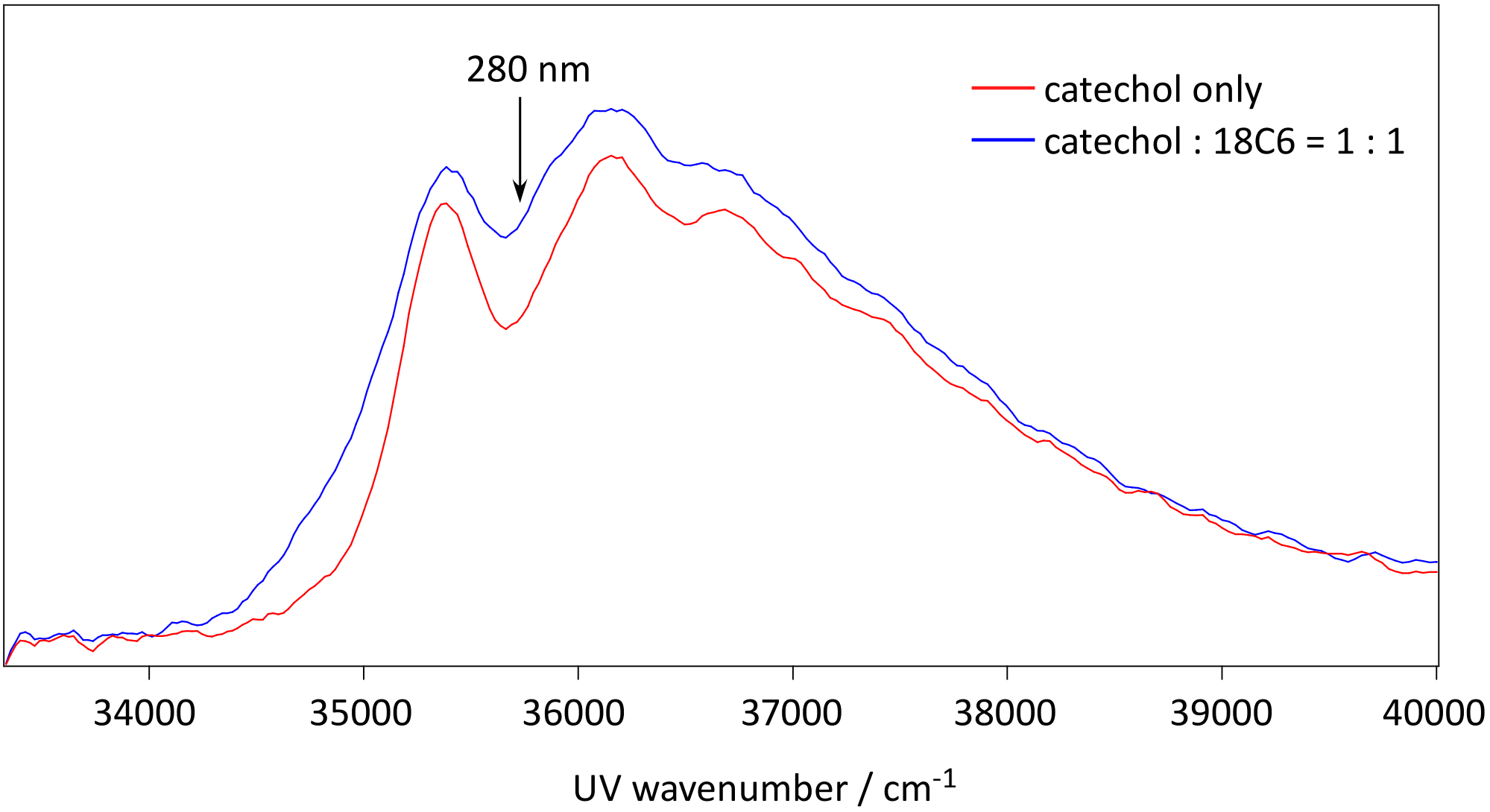
280 nm
catechol only
catechol : 18C6 = 1 : 1
34000
35000
36000
37000
38000
39000
40000
UV wavenumber / cm-1

Figure 5

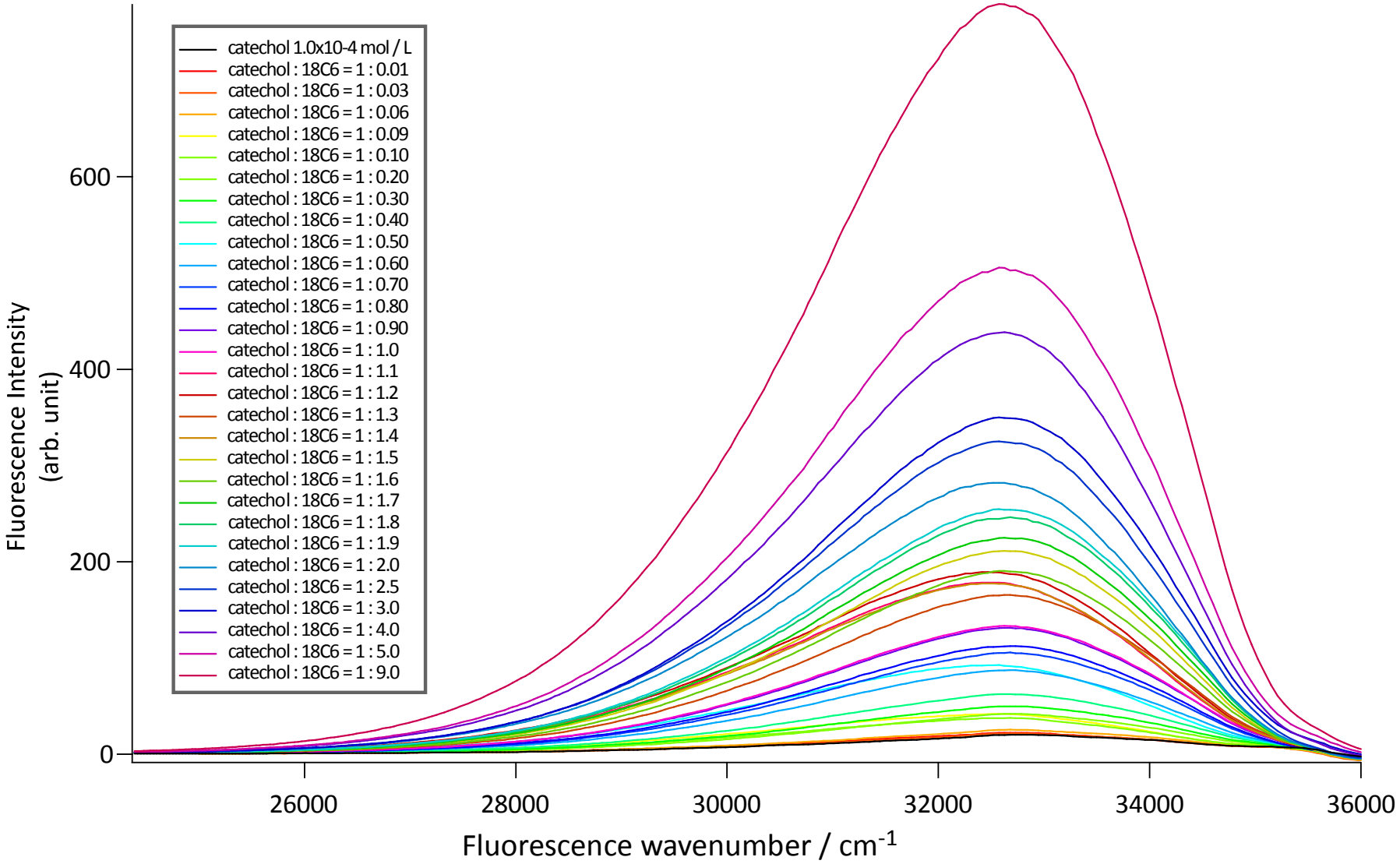
catechol 1.0x10-4 mol / L
catechol : 18C6 = 1 : 0.01
catechol : 18C6 = 1 : 0.03
catechol : 18C6 = 1 : 0.06
catechol : 18C6 = 1 : 0.09
catechol : 18C6 = 1 : 0.10
catechol : 18C6 = 1 : 0.20
catechol : 18C6 = 1 : 0.30
catechol : 18C6 = 1 : 0.40
catechol : 18C6 = 1 : 0.50
catechol : 18C6 = 1 : 0.60
catechol : 18C6 = 1 : 0.70
catechol : 18C6 = 1 : 0.80
catechol : 18C6 = 1 : 0.90
catechol : 18C6 = 1 : 1.0
catechol : 18C6 = 1 : 1.1
catechol : 18C6 = 1 : 1.2
catechol : 18C6 = 1 : 1.3
catechol : 18C6 = 1 : 1.4
catechol : 18C6 = 1 : 1.5
catechol : 18C6 = 1 : 1.6
catechol : 18C6 = 1 : 1.7
catechol : 18C6 = 1 : 1.8
catechol : 18C6 = 1 : 1.9
catechol : 18C6 = 1 : 2.0
catechol : 18C6 = 1 : 2.5
catechol : 18C6 = 1 : 3.0
catechol : 18C6 = 1 : 4.0
catechol : 18C6 = 1 : 5.0
catechol : 18C6 = 1 : 9.0
Fluorescence Intensity (arb. unit)
0
200
400
600
26000
28000
30000
32000
34000
36000
Fluorescence wavenumber / cm-1

Figure 6

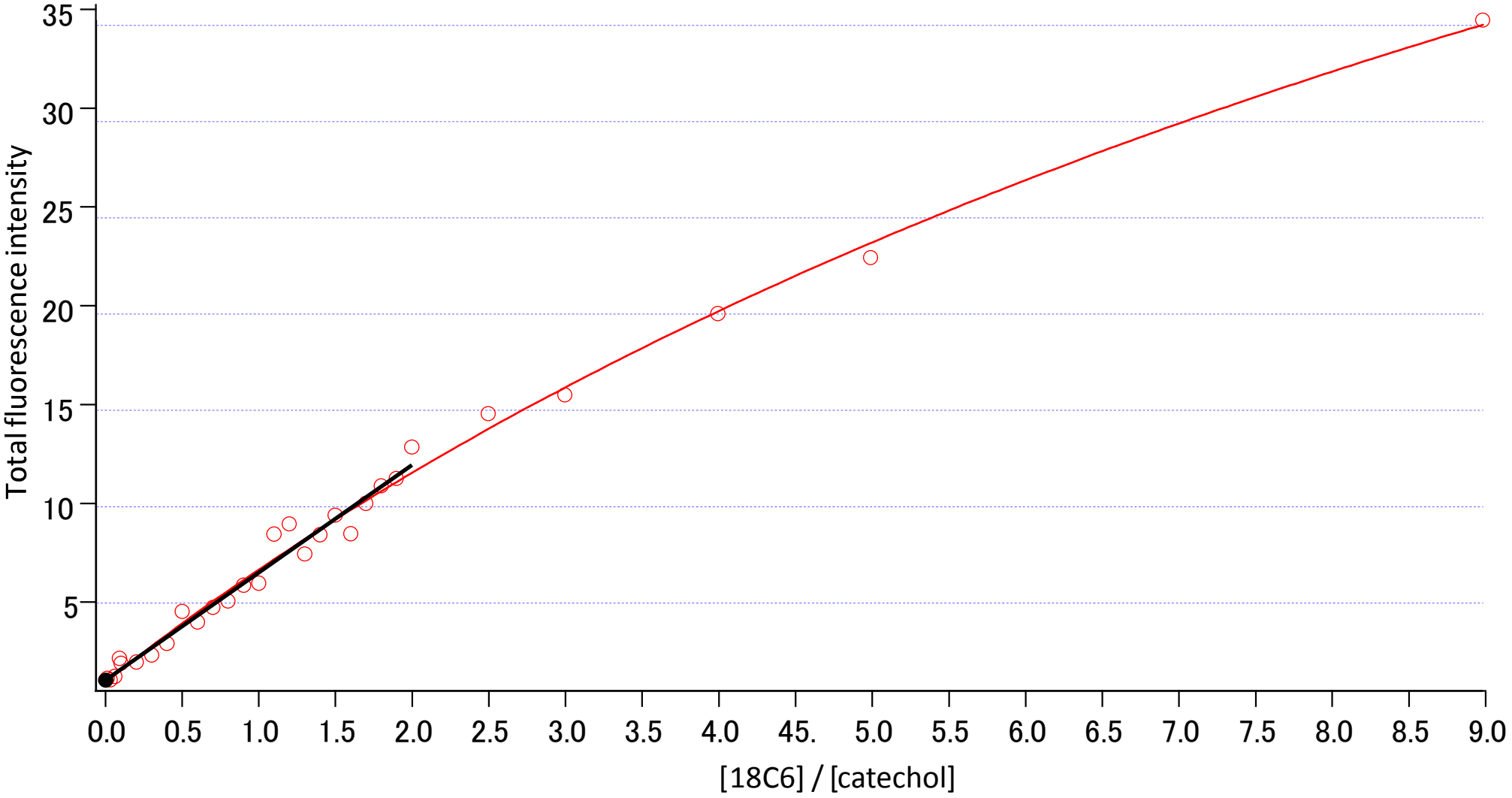
Total fluorescence intensity
35
30
25
20
15
10
5
0.0
0.5
1.0
1.5
2.0
2.5
3.0
3.5
4.0
45.
5.0
5.5
6.0
6.5
7.0
7.5
8.0
8.5
9.0
[18C6] / [catechol]

Figure 7

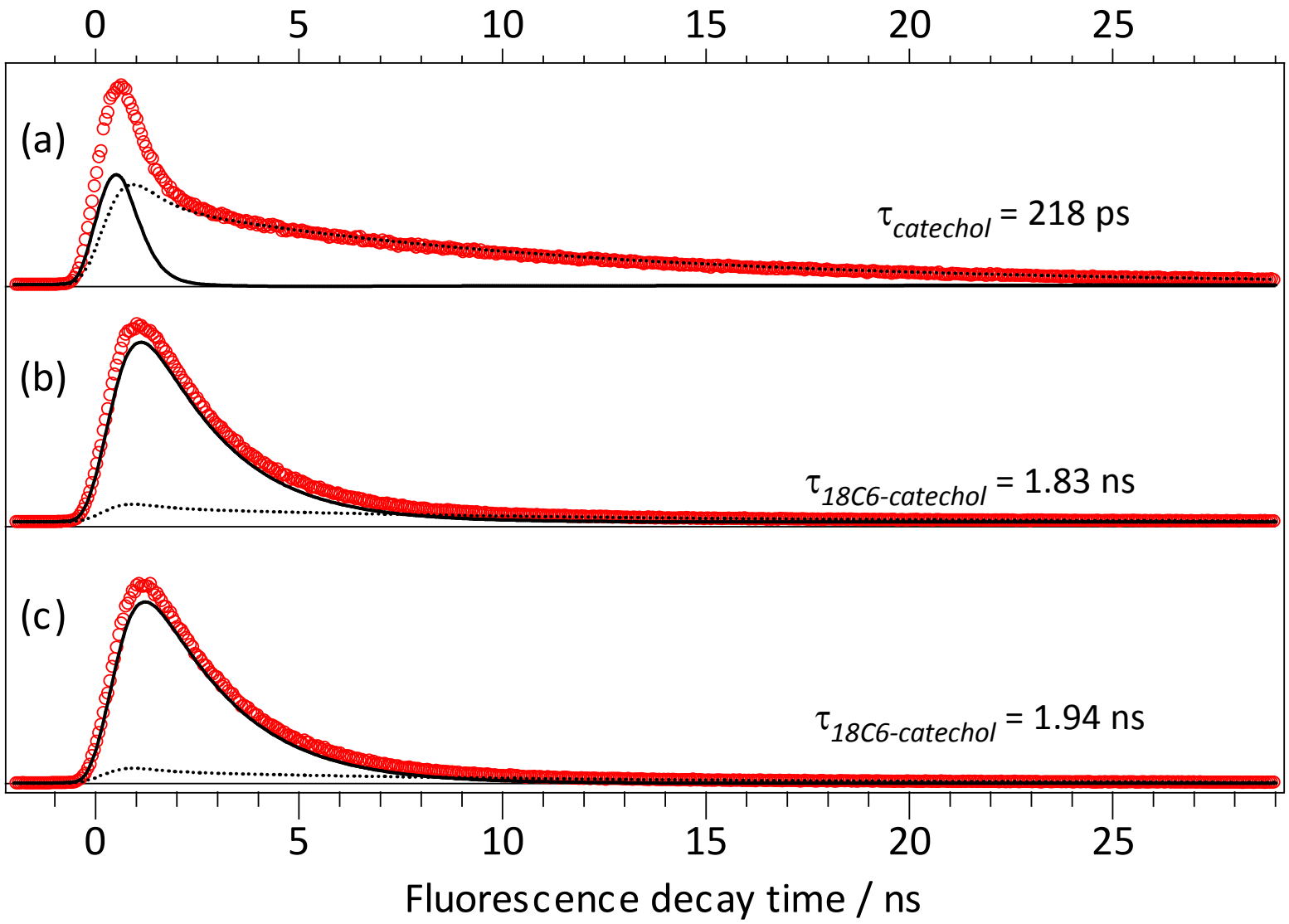
0
5
10
15
20
25
(a)
τcatechol = 218 ps
(b)
τ18C6-catechol = 1.83 ns
(c)
τ18C6-catechol = 1.94 ns
0
5
10
15
20
25
Fluorescence decay time / ns

Figure 8

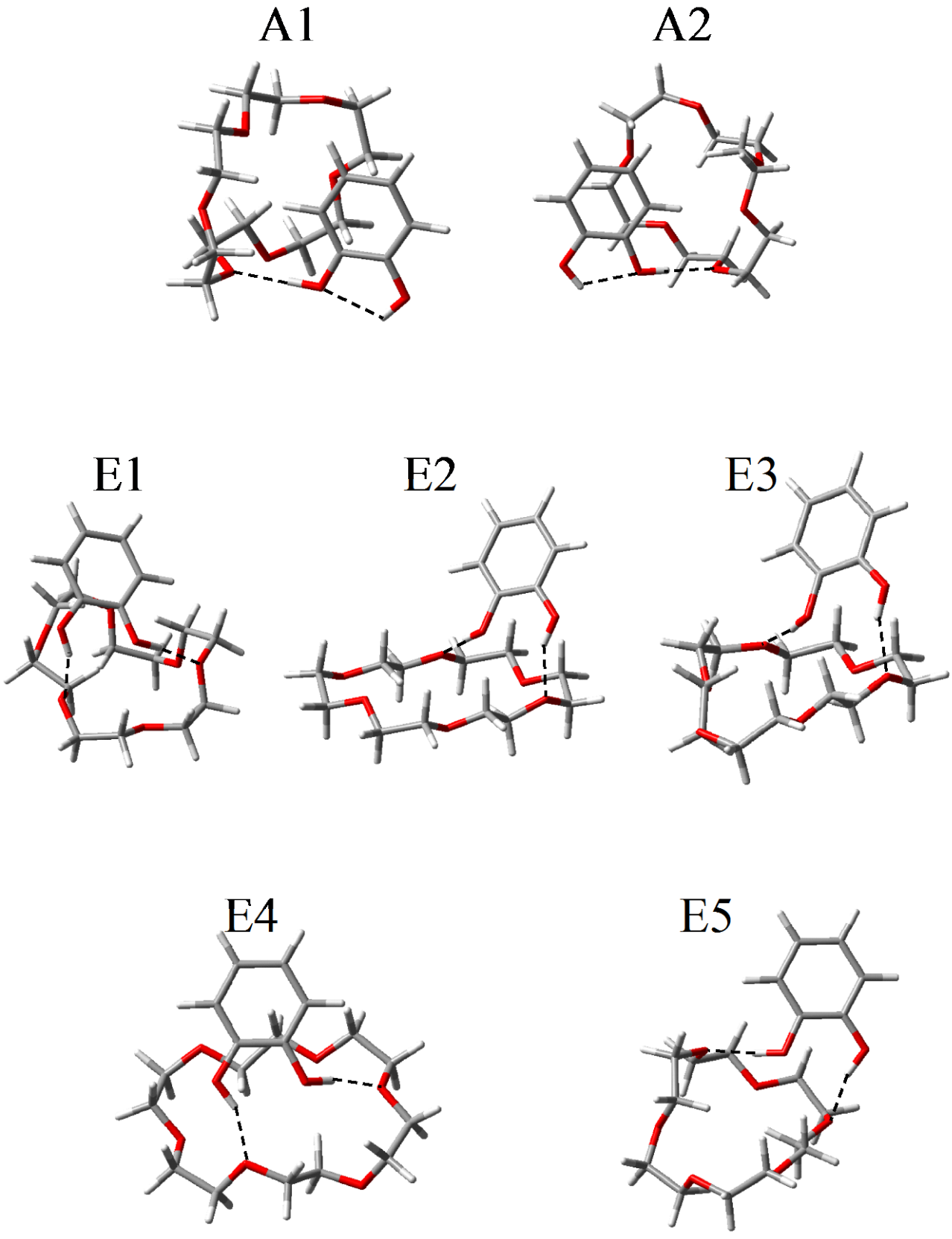

TOC